DRAFT VERSION SEPTEMBER 28, 2016
Preprint typeset using LaTeX style emulateapj v. 12/16/11

IMPLICATIONS OF SMALLER COSMIC RAY HALO AND DIFFUSION COEFFICIENT TO THE UNDERSTANDING OF THE KNEE AND OBSERVED ANISOTROPY

NIR J. SHAVIV[a,b], DAVID BENYAMIN[a], KOHTA MURASE[c,b] & TSVI PIRAN[a]
[a] Racah Institute of Physics, Hebrew University of Jerusalem, Jerusalem 91904, Israel
[b] Institute for Advanced Study, Einstein Drive, Princeton, NJ 08540, USA
[c] Dept. of Physics, Pennsylvania State University, University Park, PA 16802
Draft version September 28, 2016

ABSTRACT

Cosmic Ray diffusion models lacking nearby sources require a smaller halo and smaller diffusion coefficient in order to fit the average grammage inferred from ratios between secondary to primary cosmic rays as well as the ^{10}Be/^{9}Be which "dates" the cosmic rays. We show here that models with such modified parameters lead to a notably smaller anisotropy, releasing the tension between standard predictions and observations. For the lower diffusion coefficient, the "knee" at a few PeV is then unavoidably explained as the energy for which the Larmor radius is equal to the mean free path, because of which the ISM diffusion coefficient will increase fast above this energy (for protons). This would imply that the knee is a propagation effect and the main cosmic ray acceleration site (presumably supernova remnants) should in principle be able to accelerate up to higher energies. The smaller scales also imply that fewer sources contribute to the cosmic ray density at any given energy, giving rise to large fluctuations which can explain the anisotropy behavior above 10 TeV. Although the energy dependent composition is similar to the behavior expected in standard models, here one predicts a larger anisotropy for lighter elements at a given energy above the knee.

Subject headings: cosmic rays — anisotropy — knee

1. INTRODUCTION

Cosmic ray (CR) theories and their model parameters are often tightly constrained by a range of observations, in particular, by the measurement of the formation of secondary particles as the CRs propagate in the galactic disk and interact with the interstellar medium. Roughly speaking, the ^{10}Be fraction measurements provide a handle to the typical age of CRs, around 10^7yr. Then, in order not to overproduce the amount of stable secondary isotopes over this typical time scale, one should let the CRs diffuse out of the galactic plane, where the density is low and secondary CR production is inhibited. Namely, a typical CR diffusion halo of 1 to 4 kpc is often required. The large halo size and fixed time scale imply that the diffusion coefficient should typically be a few 10^{28} cm^2 s^{-1} at a few GeV/nuc. (e.g., Strong *et al.* 2007). In other words, the diffusion coefficient, halo size, CR age and secondary to primary ratio are intimately related.

The relatively large value of the halo size implies that "tangled" magnetic fields should exist up to distances above the galactic plane which are much larger than most gaseous components of the ISM, which only extend however up to a few 100 pc (e.g., Ferrière 2001). The required diffusion coefficient is also somewhat higher than can be expected from the typical turbulent characteristics of the ISM, which should give rise to a diffusion coefficient of typically a few 10^{27} cm^2 s^{-1} at GeV/nuc. (e.g., Strong *et al.* 2007), i.e., about an order of magnitude smaller. This smaller diffusion coefficient would require a smaller halo, but it would typically overproduce secondaries in *standard* models.

One tacit assumption in these models that bares consequences on the halo size and diffusion coefficient, however, is that the CR sources are relatively evenly distributed (Moskalenko & Strong 1998; Strong & Moskalenko 1998)—they have an azimuthally symmetric distribution around the galaxy and the local distribution is smooth as well. There are several theoretical and empirical reasons to doubt this. To begin with, most star formation in spiral armed galaxies takes place in the vicinity of spiral arms. Since core collapse SNe are the dominant type in such galaxies, most supernova remnants and presumably CR acceleration should therefore take place in the vicinity of arms (Shaviv 2003). And indeed, radio detected SNRs in spiral galaxies appear to have a clear concentration towards the arms (Lacey & Duric 2001).

It should therefore come with no surprise that the exposure ages of meteorites point to a variable cosmic ray flux (CRF). Comparison between different types of exposure ages demonstrates that the CRF over the past several million years has been higher by about 30% than the average flux over the past billion years (Lavielle *et al.* 1999), while the clustering of exposure ages is consistent with a periodically variable CRF which would naturally arise from periodic spiral arm passages (Shaviv 2002, 2003).

Besides giving rise to a time dependent CRF, the main difference between homogeneous models and those which consider the spiral arm source distribution is the *path length distribution* (PLD). The former tends to have a PLD distribution which closely resembles the inherent exponential PLD of the leaky box model (Berezinskii *et al.* 1990). The latter, on the other hand, has a PLD which is missing the short paths, giving rise to several interesting ramifications (Benyamin *et al.* 2014).

The first is implications to the halo size. Given the ^{10}Be constraint on the CR age, the amount of secondaries produced corresponds to some average ISM density with which the CRs interact. However, the CRs having short path lengths present in standard models tend to produce more secondaries as they cannot stray away from the galactic plane where the density is high, such that a given halo size produces more secondaries than it would without the short path length CRs. The observed amount of secondaries therefore requires a halo size of a few kpc. Together with the constrained age, a typical dif-

fusion coefficient of a few 10^{28} cm^2 s^{-1} is then required. On the other hand, models having a paucity of short paths do not require smaller halos to produce the same amount of secondaries. In fact, the observed production of secondaries is reproduced with a halo of only a few hundred pc and a diffusion coefficient of typically 10^{27} cm^2 s^{-1} (Benyamin *et al.* 2014). The smaller halo and diffusion coefficient are also closer to the expectations from naive diffusion models. In particular, the main components of the turbulent ISM governing the CR diffusion are concentrated to within about 100 pc from the plane (e.g., Kim *et al.* 2013). It would also explain why indirect inference of the cosmic ray density point to a small halo as well (Shaviv *et al.* 2014)[1].

The PLD of the spiral armed model has additional ramifications. Since higher energy CRs diffuse out of the galaxy faster, they have a lower probability of producing secondaries, which is why the secondary to primary ratio should decrease with energy. However, the PAMELA satellite detected a clear rise in the supposedly secondary positrons to primary electron ratio above 10 GeV (Adriani 2009). Although there are many explanations in the literature, it was shown that having the CR sources concentrated in the spiral arms naturally reproduces the rise without any free parameters (Shaviv *et al.* 2009). This is because the paucity of short path lengths implies that primary energetic electrons cool before reaching the solar system, while secondary positrons can form in the solar vicinity. The different PLD also explains the production of heavy secondaries relative to the production of light ones Benyamin *et al.* (2016).

Seemingly unrelated are additional aspects of cosmic rays at higher energies, the most notable of which is the "knee" at $\sim 3\times10^{15}$eV. At this energy, there is a steepening of the cosmic ray spectrum and a progressive change from a composition which is primarily that of protons to primarily Iron. The knee is generally explained as the maximal energy to which CRs can be accelerated by SNRs. Since a given magnetic field and source size can accelerate to energies of $E\sim ZeBR$, also known as the Hillas criterion (Hillas 1984), one expects that higher Z species will be accelerated to higher energies by the same sources, up to energies which are a factor of Z higher. In addition, since CRs arriving at the solar system come from a number of sources, one of the interesting aspects that the standard explanation for the knee should satisfy is that different sources should have roughly the same maximal energy or else the associated "knee" would be smeared, or alternatively, be dominated by one source (Erlykin & Wolfendale 1997).

The second important aspect of cosmic ray measurements at energies below the knee is their detectable anisotropy. Measurements reveal a non-monotonic behavior of the anisotropy, ranging between 10^{-4} to 10^{-3} over the 100 GeV to 300 TeV range (e.g. Aartsen *et al.* 2013; Abbasi *et al.* 2012; Abdo *et al.* 2009; Aglietta *et al.* 2009, 1996; Amenomori *et al.* 2005; Antoni *et al.* 2004; Gerhardy & Clay 1983; Kifune *et al.* 1986, and see fig. 1 as well). An anisotropy is expected if there is a gradient in the cosmic ray distribution (e.g., Ginzburg & Syrovatskii 1964), effects related to the local magnetic field (e.g., Mertsch & Funk 2015), and also a contribution from a motion of the solar system relative to the local standard of rest (Compton & Getting 1935).

We show in the present work that the smaller halo and diffusion coefficients are also consistent with additional aspects pertaining to higher energy cosmic rays. In §2 we show that in a model having a smaller diffusion coefficient together with a Kolmogorov structure spectrum arising from turbulence, one expects the Larmor radius to be comparable to the diffusion mean free path at the observed cosmic ray knee. We also show that the same parameters recover the observed behavior of the anisotropy. This is done analytically in §3, and numerically in §4. We end with a discussion in §5.

2. THE KNEE IN INHOMOGENEOUS MODELS WITH SMALLER HALO AND D

As mentioned above, inhomogeneous models require a halo of only a few hundred pc, and a diffusion coefficient which is typically one order of magnitude smaller than standard "homogeneous" models. The smaller diffusion coefficient, and in particular, the smaller mean free path associated with it, has a very interesting implication.

Standard cosmic ray diffusion model generally predict that the power-law behavior of the diffusion coefficient will increase at the energy for which the mean free path is comparable to the Larmor radius. For a diffusion in an ISM described with a Kolmogorov spectrum one expects the diffusion coefficient to go as $D\propto(E/Z)^{1/3}$ below the aforementioned transition energy $E_{\rm trans}$, while it should behave as $D\propto E^2$ above (Aloisio & Berezinsky 2004; Parizot 2004).

By comparing the Larmor gyration radius $r_l=E/ZeB$ to the mean free path $\ell=3D(E)/c$, we find

$$\begin{aligned}E_{\rm trans}&=6.25\times10^{11}{\rm eV}\;625^{\frac{p}{1-p}}48^{\frac{1}{1-p}}\left(\frac{B}{1\mu G}\right)^{\frac{1}{1-p}}\\&\times\left(\frac{D_0}{10^{27}{\rm cm^2/s}}\right)^{\frac{1}{1-p}}Z\\&=5.5\times10^{15}{\rm eV}\left(\frac{B}{1\mu G}\right)^{\frac{3}{2}}\left(\frac{D_0}{10^{27}{\rm cm^2/s}}\right)^{\frac{3}{2}}Z\end{aligned}\quad(1)$$

where we have assumed a diffusion law of the form $D=D_0\,(E/Z\;{\rm GeV})^p$, and $p=1/3$ for the second expression, as would be expected for a Kolmogorov turbulence.

Clearly, models with small halos and diffusion coefficients give rise to a knee-like power law break at a few PeV, as is observed. But this also requires the diffusion index to be 1/3. Any larger value will push the knee to higher energies.

Another interesting feature is that the power law breaks for species with higher Z's, is at progressively higher energies. Similar behavior is predicted in the standard explanation for the knee, that it is the highest typical energy to which the galactic CR accelerators can accelerate. Hillas' criterion (Hillas 1984) gives that the maximal energy is $E_{\rm max}=ZeBR$. Namely, the knee in both type of models increase linearly with Z. This is not surprising given since all length scales in the two problems depend on E/Z only, nor that it has been experimentally observed (Apel *et al.* 2011). However, as we discuss below, there will be a difference in the *composition* dependent anisotropy.

3. ANISOTROPY IN INHOMOGENEOUS MODELS WITH SMALLER HALO AND D

The naive expectation of having a smaller halo size is a higher anisotropy, however, the smaller halo size requires also a smaller diffusion coefficient, which more than compensates.

[1] Given the smaller scale it is probably not appropriate to call the CR diffusion regions a "halo" at all, though we will adhere to the terminology. Moreover, the small halo does not preclude the existence of a larger more tenuous halo provided that its CR "optical depth" does not dominate the smaller diffusion region.

The anisotropy from a gradient in the number density of cosmic rays is expected to be (e.g., Ginzburg & Syrovatskii 1964)

$$\mathcal{A} \equiv \frac{\phi_{\rm max} - \phi_{\rm min}}{\phi_{\rm max} + \phi_{\rm min}} = \frac{3D}{c}\frac{\nabla n}{n} \approx \frac{\ell}{h}, \quad (2)$$

where $\ell = 3D/c$ is the effective mean free path of the diffusion process, and also consider that the typical length scale of the gradient is h, the halo size.

To further constrain the anisotropy, we need to relate the mean free path or equivalently the diffusion coefficient, with the halo size. This can be done by considering that the diffusion time scale is empirically constrained to be about $\tau_{\rm GeV} \sim 10^7$ yr at 1 GeV using ^{10}Be measurements (e.g., Strong *et al.* 2007). Since

$$\tau(E) \sim \frac{h^2}{3D(E)} \quad (3)$$

one then finds that for a 1/3 power law index, the anisotropy comes out to be

$$\mathcal{A} \sim \frac{h}{\tau(E)c} \sim 10^{-3}\frac{h}{300{\rm pc}}\left(\frac{E}{\rm TeV}\right)^{1/3}. \quad (4)$$

Thus, for a fixed CR age, the size of the anisotropy scales as the halo size. A smaller halo gives an anisotropy which is consistent with the observations (see fig. 1).

In models which have an inhomogeneous source distribution, the distance to the nearest spiral arm is an additional distance scale playing a role, and it is the smaller of the scales which will dominate the anisotropy. However, Benyamin *et al.* (2014) have shown that both are of order a few hundred pc.

Another interesting aspect of the smaller halo which pertains to the expected anisotropy is the expected size of the fluctuations. The smaller diffusion coefficient and halo size implies that the number of SNR from which cosmic rays can reach us is smaller. As a consequence, the expected Poisson fluctuations are correspondingly larger. If $\mathcal{R}_{\rm local}$ is the local rate of supernovae per unit area of the galactic disk, then the number of sources at a given energy is roughly

$$n_{\rm sources} \sim \pi\mathcal{R}_{\rm local}h^2\tau_E \sim 12\left(\frac{h}{300{\rm pc}}\right)^2\left(\frac{E}{\rm TeV}\right)^{1/3} \quad (5)$$

where we have taken an overall galactic rate of a SN per 30 years, and exponential decay of 4 kpc in their distribution.

We therefore expect variations $1/\sqrt{n_{sources}}$ which are of order 25% at a TeV, simply due to the smaller volume having fewer CR sources. In standard models, the number of sources scales as h^2 and therefore the variations in the anisotropy are a factor of $1/h$ smaller, or 2-8% at a TeV, for typical values found in the literature.

4. SIMULATING THE ANISOTROPY

Instead of estimating the anisotropy analytically, as given by eq. 4, we can also simulate it by generating many realizations. This allows not only to study the average anisotropy, but more robustly estimate the size of the fluctuations. Moreover, actual realizations can be compared to the observations, to see whether or not the model is consistent.

We start by using the results of the nominal model of Benyamin *et al.* (2014). This gives the local gradients in the sources and CRs. Then, we can make many realizations while assuming that the overall Milky Way supernova rate is 1 per 30 years. We assume that each SNR instantaneously injects a δ-function of CRs, which initially diffuses. Since the boundary conditions for the diffusion process are that the CR density vanishes at $z = \pm h$, we assume that the CR density at location $\mathbf{r}$ and time t from a supernova that took place at $\mathbf{r_0}$ and t_0 is given by

$$n_1(\mathbf{r}, t, \mathbf{r_0}, t_0, E) = \quad (6)$$

$$\begin{cases} \frac{1}{(4\pi Dt)^{3/2}}\exp\left(-\frac{(\mathbf{r}-\mathbf{r_0})^2}{4Dt}\right) & \text{for } t \le (fh)^2/D \\ \frac{1}{4\pi hDt}\exp\left(-\frac{(x-x_0)^2+(y-y_0)^2}{4Dt}\right)\times & \\ \sum_{i=1}^{i_{max}}\sin\left(\frac{\pi(z_0+h)i}{2h}\right)\sin\left(\frac{\pi(z+h)i}{2h}\right)\exp\left(-D\left(\frac{\pi i}{2h}\right)^2 t\right) & \text{for } t > (fh)^2/D \end{cases}$$

The accurate solution is the second expression with $i_{max} \to \infty$, obtained obtained through a Fourier series expansion. If however we take only a finite number of terms, then the short time solution is more accurately given by the first expression. We take $i_{max} = 5$ and $f = 0.2$, which gives very accurate solutions as long as $|z|, |z_0| \lesssim 0.4h$. Note also that the dependence on energy enters through $D = D(E)$, which we assume to be $D_0(E/E_0)^{1/3}$.

The single SN distribution can then be summed over assuming an average distribution given by Benyamin *et al.* (2014).

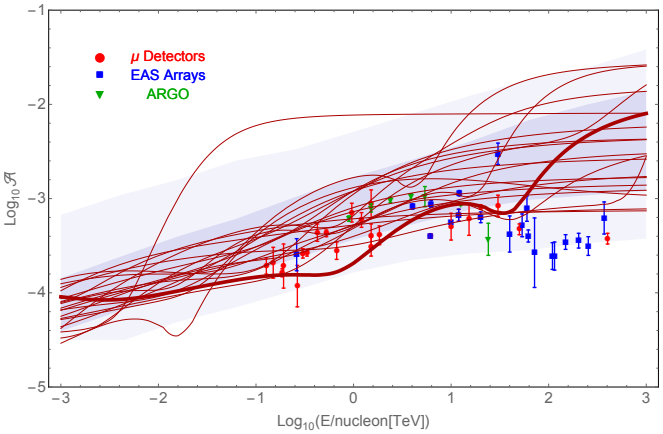

FIG. 1.— The anisotropy as a function of energy. The red lines are 20 random realizations of the model described in the text. One is denoted with a heavy line as an example with variations similar to the experimental measurements denoted with the points (Aartsen *et al.* 2013; Abbasi *et al.* 2012; Abdo *et al.* 2009; Aglietta *et al.* 2009, 1996; Amenomori *et al.* 2005; Antoni *et al.* 2004; Gerhardy & Clay 1983; Kifune *et al.* 1986, color coded according to the detector type). At a given energy, there is a 31.7% probability (i.e., 1 σ) that the anisotropy will be outside the darker region, and 5% outside the lighter region. There is however a 70% change that it would leave the dark band at *any* energy, or 14% chance it would leave the lighter region. This is calculated based on 1000 realizations. The solid green line is the expectation from the nominal model parameters, $D = 6\times10^{26}{\rm cm}^2/{\rm s}$ at 1 GeV, $h = 250pc$ and $p = 1/3$, and using eq. 4. The short and long dashed lines denote the anisotropy expected from nominal models of Strong & Moskalenko (1998), having $D = 5\times10^{28}{\rm cm}^2/{\rm s}$ at 1 GeV, $h = 7.7kpc$ and $p = 1/3$ (short dashed) and $D = 10^{29}{\rm cm}^2/{\rm s}$ at 1 GeV, $h = 5kpc$ and $p = 0.6$ (long dashed). The dotted horizontal line is the expected anisotropy from the motion of the solar system relative to the local standard of rest (Compton & Getting 1935).

The results of 10^3 realizations is given in fig. 1. We find that due to the finite number of sources, the expected variation from one realization to another is relatively large. The

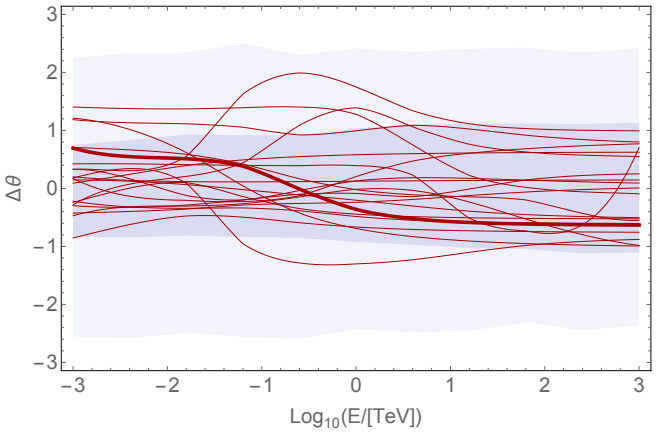

FIG. 2.— The angle difference between the direction of the average SN gradient and the actual direction of the anisotropy in the different realizations. The lines and shaded regions are the same as in fig. 1. In particular, the heavy red line is of the same realization. Note however that although the regions are defined to have the same local probability (i.e., for a given energy), because of the larger correlation in energy, the probability for a realization to leave the regions for *any* energy is lower, being 60% and 7% instead.

darker/lighter gray bands respectively describe the regions for which there is a 31.7% (i.e., 1-σ) or 5% chance that the anisotropy *at a given energy* will be larger outside the region. The total 1-σ region is about 0.5 dex wide at 1 TeV. If we ask the question what is the probability that it will be outside the band at *any* energy, the probabilities are respectively 70% and 14%. Since the minimum observed anisotropy is slightly below the lighter band, there is a 10% probability for such a realization to arise (or 5% for a one sided probability). Namely, the decrease in anisotropy between 10 to 100 TeV is not very likely but still a plausible outcome of the model.

Fig. 2 depicts the difference between the direction of gradient of the CR sources, and the actual gradient in the CR distribution, as obtained in the model for different realizations. Interestingly, variations as large as 1 radian are frequently expected, and a large "swing" in the direction is too possible. For example, the sample realization emphasized in the figure (exhibiting an anisotropy dip similar to the observation) that also has a swing of about a radian, with other realizations having even larger swings, similar to the measurements showing a large change in the direction as the CR energy is increased (e.g., see Di Sciascio & Iuppa 2013).

5. DISCUSSION AND SUMMARY

Our starting point in this work is a cosmic ray diffusion model which assumes that the CR sources are not distributed with an azimuthally symmetric distribution, but instead have the sources concentrated towards the arms. This is expected given that most SNe in the Milky Way are core collapse.

In order for the model to fit the various measurements of secondaries and primary CRs, it needs a smaller diffusion coefficient and a smaller halo.

We have shown here that without any additional parameter fitting, the nominal model parameters of Benyamin *et al.* (2014) automatically recover the following:

1. The "knee" at a few PeV. It is the energy for which the Larmor radius of protons is the same as the mean free path associated with the diffusion.

2. The second knee at almost 100 PeV is then immediately explained as the equivalent Iron "knee", predicted to be at an energy 26 times higher. This is similar to standard models which have the same Z dependence.

3. The size of the anisotropy is smaller than standard models, and similar to the observations.

4. The smaller number of CR sources gives rise to larger fluctuations from one realization to another. It explains the irregular behavior of the anisotropy as a function of energy and it explains the directional swings with energy.

One of the interesting implications of the model is that the knee should not be associated with the maximal energy which the galactic CR sources can accelerate. A more reasonable assumption would be that different the different sources, presumably supernova remnants can accelerate up to different energies, perhaps as a function of time, such that when they are added up, one obtains a featureless spectrum which is only modified by the propagation feature. Moreover, because the propagation feature depends only on the local magnetic field, it explains why it is so much sharper than could be expected if the knee was due to cosmic rays coming from a diverse population of supernova remnants.

Another qualitative difference exists if the knee is due to a break in the diffusion coefficient. Such a break would imply that the anisotropy should rise faster above the knee than expected if the knee is due to a maximal acceleration energy. Moreover, given that different species have knees at different energies, one would expect the anisotropy to be *specie dependent*—with protons increasing their anisotropy already from the knee, and heavier elements at higher energies. This prediction could be used to distinguish between the models.

ACKNOWLEDGEMENTS

NJS gratefully acknowledges the support of the IBM Einstein Fellowship and Israel Science Foundation (grant no. 1423/15). This research project was also supported by the I-CORE Program of the Planning and Budgeting Committee and the Israel Science Foundation (center 1829/12).

REFERENCES

Aartsen, M. G., Abbasi, R., Abdou, Y., Ackermann, M., Adams, J., Aguilar, J. A., Ahlers, M., Altmann, D., Andeen, K., Auffenberg, J., & et al. 2013. Observation of Cosmic-Ray Anisotropy with the IceTop Air Shower Array. *ApJ*, **765**, 55.

Abbasi, R., Abdou, Y., Abu-Zayyad, T., Ackermann, M., Adams, J., Aguilar, J. A., Ahlers, M., Allen, M. M., Altmann, D., Andeen, K., & et al. 2012. Observation of Anisotropy in the Galactic Cosmic-Ray Arrival Directions at 400 TeV with IceCube. *ApJ*, **746**, 33.

Abdo, A. A., Allen, B. T., Aune, T., Berley, D., Casanova, S., Chen, C., Dingus, B. L., Ellsworth, R. W., Fleysher, L., Fleysher, R., Gonzalez, M. M., Goodman, J. A., Hoffman, C. M., Hopper, B., Hüntemeyer, P. H., Kolterman, B. E., Lansdell, C. P., Linnemann, J. T., McEnery, J. E., Mincer, A. I., Nemethy, P., Noyes, D., Pretz, J., Ryan, J. M., Parkinson, P. M. S., Shoup, A., Sinnis, G., Smith, A. J., Sullivan, G. W., Vasileiou, V., Walker, G. P., Williams, D. A., & Yodh, G. B. 2009. The Large-Scale Cosmic-Ray Anisotropy as Observed with Milagro. *ApJ*, **698**, 2121–2130.

Adriani, O. et al. 2009. An anomalous positron abundance in cosmic rays with energies 1.5-100GeV. *Nature*, **458**, 607–609.

Aglietta, M., Alessandro, B., Antonioli, P., Arneodo, F., Bergamasco, L., Bertaina, M., Bosio, A., Castellina, A., Castagnoli, C., Chiavassa, A., Cini Castagnoli, G., D'Ettorre Piazzoli, B., di Sciascio, G., Fulgione, W., Galeotti, P., Ghia, P. L., Iacovacci, M., Mannocchi, G., Melagrana, C., Mengotti Silva, N., Morello, C., Navarra, G., Riccati, L., Saavedra, O., Trinchero, G. C., Vallania, P., Vernetto, S., & EAS-Top Collaboration. 1996. A Measurement of the Solar and Sidereal Cosmic-Ray Anisotropy at E 0 approximately 10 14 eV. *ApJ*, **470**, 501.

Aglietta, M., Alekseenko, V. V., Alessandro, B., Antonioli, P., Arneodo, F., Bergamasco, L., Bertaina, M., Bonino, R., Castellina, A., Chiavassa, A., D'Ettorre Piazzoli, B., Di Sciascio, G., Fulgione, W., Galeotti, P., Ghia, P. L., Iacovacci, M., Mannocchi, G., Morello, C., Navarra, G., Saavedra, O., Stamerra, A., Trinchero, G. C., Valchierotti, S., Vallania, P., Vernetto, S., & Vigorito, C. 2009. Evolution of the Cosmic-Ray Anisotropy Above 10^{14} eV. *ApJ*, **692**, L130–L133.

Aloisio, R., & Berezinsky, V. 2004. Diffusive Propagation of Ultra-High-Energy Cosmic Rays and the Propagation Theorem. *ApJ*, **612**, 900–913.

Amenomori, M., Ayabe, S., Cui, S. W., Danzengluobu, Ding, L. K., Ding, X. H., Feng, C. F., Feng, Z. Y., Gao, X. Y., Geng, Q. X., Guo, H. W., He, H. H., He, M., Hibino, K., Hotta, N., Hu, H., Hu, H. B., Huang, J., Huang, Q., Jia, H. Y., Kajino, F., Kasahara, K., Katayose, Y., Kato, C., Kawata, K., Labaciren, Le, G. M., Li, J. Y., Lu, H., Lu, S. L., Meng, X. R., Mizutani, K., Mu, J., Munakata, K., Nagai, A., Nanjo, H., Nishizawa, M., Ohnishi, M., Ohta, I., Onuma, H., Ouchi, T., Ozawa, S., Ren, J. R., Saito, T., Sakata, M., Sasaki, T., Shibata, M., Shiomi, A., Shirai, T., Sugimoto, H., Takita, M., Tan, Y. H., Tateyama, N., Torii, S., Tsuchiya, H., Udo, S., Utsugi, T., Wang, B. S., Wang, H., Wang, X., Wang, Y. G., Wu, H. R., Xue, L., Yamamoto, Y., Yan, C. T., Yang, X. C., Yasue, S., Ye, Z. H., Yu, G. C., Yuan, A. F., Yuda, T., Zhang, H. M., Zhang, J. L., Zhang, N. J., Zhang, X. Y., Zhang, Y., Zhang, Y., Zhaxisangzhu, Zhou, X. X., & Tibet Asγ Collaboration. 2005. Large-Scale Sidereal Anisotropy of Galactic Cosmic-Ray Intensity Observed by the Tibet Air Shower Array. *ApJ*, **626**, L29–L32.

Antoni, T., Apel, W. D., Badea, A. F., Bekk, K., Bercuci, A., Blümer, H., Bozdog, H., Brancus, I. M., Büttner, C., Daumiller, K., Doll, P., Engel, R., Engler, J., Fessler, F., Gils, H. J., Glasstetter, R., Haungs, A., Heck, D., Hörandel, J. R., Kampert, K.-H., Klages, H. O., Maier, G., Mathes, H. J., Mayer, H. J., Milke, J., Müller, M., Obenland, R., Oehlschläger, J., Ostapchenko, S., Petcu, M., Rebel, H., Risse, A., Risse, M., Roth, M., Schatz, G., Schieler, H., Scholz, J., Thouw, T., Ulrich, H., van Buren, J., Vardanyan, A., Weindl, A., Wochele, J., Zabierowski, J., & KASCADE Collaboration. 2004. Large-Scale Cosmic-Ray Anisotropy KASCADE. *ApJ*, **604**, 687–692.

Apel, W. D., Arteaga-Velázquez, J. C., Bekk, K., Bertaina, M., Blümer, J., Bozdog, H., Brancus, I. M., Buchholz, P., Cantoni, E., Chiavassa, A., Cossavella, F., Daumiller, K., de Souza, V., Di Pierro, F., Doll, P., Engel, R., Engler, J., Finger, M., Fuhrmann, D., Ghia, P. L., Gils, H. J., Glasstetter, R., Grupen, C., Haungs, A., Heck, D., Hörandel, J. R., Huber, D., Huege, T., Isar, P. G., Kampert, K.-H., Kang, D., Klages, H. O., Link, K., Łuczak, P., Ludwig, M., Mathes, H. J., Mayer, H. J., Melissas, M., Milke, J., Mitrica, B., Morello, C., Navarra, G., Oehlschläger, J., Ostapchenko, S., Over, S., Palmieri, N., Petcu, M., Pierog, T., Rebel, H., Roth, M., Schieler, H., Schröder, F. G., Sima, O., Toma, G., Trinchero, G. C., Ulrich, H., Weindl, A., Wochele, J., Wommer, M., & Zabierowski, J. 2011. Kneelike Structure in the Spectrum of the Heavy Component of Cosmic Rays Observed with KASCADE-Grande. *Phys. Rev. Lett.*, **107**, 171104.

Benyamin, D., Nakar, E., Piran, T., & Shaviv, N. J. 2014. Recovering the Observed B/C Ratio in a Dynamic Spiral-armed Cosmic Ray Model. *ApJ*, **782**, 34.

Benyamin, D., Nakar, E., Piran, T., & Shaviv, N. J. 2016. The B/C and Sub-iron/Iron Cosmic Ray Ratios—Further Evidence in Favor of the Spiral-Arm Diffusion Model. *ApJ*, **826**, 47.

Berezinskii, V. S., Bulanov, S. V., Dogiel, V. A., & Ptuskin, V. S. 1990. *Astrophysics of cosmic rays*.

Compton, Arthur H., & Getting, Ivan A. 1935. An Apparent Effect of Galactic Rotation on the Intensity of Cosmic Rays. *Phys. Rev.*, **47**, 817–821.

Di Sciascio, G., & Iuppa, R. 2013. *Homage to the discovery of Cosmic Rays*. Nova Science Publishers. Chap. 9 - On the Observation of the Cosmic Ray Anisotropy below 10^{15} eV, eprint arXiv:1407.2144.

Erlykin, A. D., & Wolfendale, A. W. 1997. A single source of cosmic rays in the range ? - ? eV. *Journal of Physics G Nuclear Physics*, **23**, 979–989.

Ferrière, K. M. 2001. The interstellar environment of our galaxy. *Reviews of Modern Physics*, **73**, 1031–1066.

Gerhardy, P. R., & Clay, R. W. 1983. Southern hemisphere cosmic-ray anisotropy at 10^{16} eV. *Journal of Physics G Nuclear Physics*, **9**, 1279–1287.

Ginzburg, V. L., & Syrovatskii, S. I. 1964. *The Origin of Cosmic Rays*.

Hillas, A. M. 1984. The Origin of Ultra-High-Energy Cosmic Rays. *ARA&A*, **22**, 425–444.

Kifune, T., Hara, T., Hatano, Y., Hayashida, N., Honda, M., Kamata, K., Nagano, M., Nishijima, K., Tanahashi, G., & Teshima, M. 1986. Anisotropy of the arrival direction of extensive air showers observed at Akeno. *Journal of Physics G Nuclear Physics*, **12**, 129–142.

Kim, C.-G., Ostriker, E. C., & Kim, W.-T. 2013. Three-dimensional Hydrodynamic Simulations of Multiphase Galactic Disks with Star Formation Feedback. I. Regulation of Star Formation Rates. *ApJ*, **776**, 1.

Lacey, C. K., & Duric, N. 2001. Cosmic-Ray Production and the Role of Supernovae in NGC 6946. *ApJ*, **560**, 719–729.

Lavielle, B., Marti, K., Jeannot, J.-P., Nishiizumi, K., & Caffee, M. 1999. The ^{36}Cl- ^{36}Ar- ^{40}K- ^{41}K records and cosmic ray production rates in iron meteorites. *Earth and Planetary Science Letters*, **170**, 93–104.

Mertsch, Philipp, & Funk, Stefan. 2015. Solution to the Cosmic Ray Anisotropy Problem. *Phys. Rev. Lett.*, **114**, 021101.

Moskalenko, I. V., & Strong, A. W. 1998. Production and Propagation of Cosmic-Ray Positrons and Electrons. *ApJ*, **493**, 694.

Parizot, E. 2004. GZK horizon and magnetic fields. *Nuclear Physics B Proceedings Supplements*, **136**, 169–178.

Shaviv, N. J. 2002. Cosmic Ray Diffusion from the Galactic Spiral Arms, Iron Meteorites, and a Possible Climatic Connection. *Physical Review Letters*, **89**(5), 051102.

Shaviv, N. J. 2003. The spiral structure of the Milky Way, cosmic rays, and ice age epochs on Earth. *New Astron.*, **8**, 39–77.

Shaviv, N. J., Nakar, E., & Piran, T. 2009. Inhomogeneity in Cosmic Ray Sources as the Origin of the Electron Spectrum and the PAMELA Anomaly. *Physical Review Letters*, **103**(11), 111302.

Shaviv, N. J., Prokoph, A., & Veizer, J. 2014. Is the Solar System's Galactic Motion Imprinted in the Phanerozoic Climate? *Scientific Reports*, **4**, 6150.

Strong, A. W., & Moskalenko, I. V. 1998. Propagation of Cosmic-Ray Nucleons in the Galaxy. *ApJ*, **509**, 212–228.

Strong, A. W., Moskalenko, I. V., & Ptuskin, V. S. 2007. Cosmic-Ray Propagation and Interactions in the Galaxy. *Annual Review of Nuclear and Particle Science*, **57**, 285–327.